Supplemental Document

Optics Letters

# Design of broadband and wide-field-of-view metalenses: supplement

FAN YANG,[1,5] SENSONG AN,[2] MIKHAIL Y. SHALAGINOV,[1] HUALIANG ZHANG,[2] CLARA RIVERO-BALEINE,[3] JUEJUN HU,[1,4] AND TIAN GU[1,4,*]

[1]*Department of Materials Science & Engineering, Massachusetts Institute of Technology, Cambridge, Massachusetts 02139, USA*
[2]*Department of Electrical & Computer Engineering, University of Massachusetts Lowell, Lowell, Massachusetts 01854, USA*
[3]*Lockheed Martin Corporation, Orlando, Florida 32819, USA*
[4]*Materials Research Laboratory, Massachusetts Institute of Technology, Cambridge, Massachusetts 02139, USA*
[5]*e-mail: yangf@mit.edu*
[*]*Corresponding author: gutian@mit.edu*



Supplement DOI: https://doi.org/10.6084/m9.figshare.16895758

Parent Article DOI: https://doi.org/10.1364/OL.439393

# Design of broadband and wide field-of-view metalenses: supplemental document

## 1. EXAMPLES OF META-ATOM STRUCTURES

6 meta-atoms are randomly selected from the 3000 meta-atom library, and their top-view layouts as well as amplitude and phase responses are shown in Fig. S1.

## 2. DIRECT SEARCH (DS) ALGORITHM FOR OPTIMIZATION

DS optimization is combined with deep learning algorithm to perform broadband and wide field-of-view (FOV) metalenses design. While deep learning algorithm generates free-form meta-atom structures with diverse dispersion characteristics, DS algorithm optimizes phase and amplitude profiles on metasurface by controlling distribution of meta-atoms to obtain target functionalities. The flow chart of the DS algorithm is shown in Fig. S2. It optimizes a pre-defined figure-of-merit (FOM) that characterizes performance of the optical system.

For our first example of the achromatic metalens, the FOM is defined as:

$$FOM = \sum_i I_{\lambda(i)} - \kappa \cdot S^2\{I_{\lambda(i)}\} \tag{S1}$$

$I_{\lambda(i)}$ is the intensity at the target focal spot position ($f$ = 400 $\mu$m on the optical axis) at wavelength $\lambda(i)$, and the summation is performed over the spectral range 1-1.5 $\mu$m with 0.01 $\mu$m sampling spacing. $S^2\{I_{\lambda(i)}\}$ is the variance of the sampled intensities, and a negative sign is assigned to limit the variance of the metalens performance across different wavelengths. $\kappa$ is a coefficient empirically set to 0.5 to seek a balance between the average performance across the spectral range and the variance among them.

For the broadband wide-FOV metalens design, the FOM is defined as:

$$FOM = \sum_{i,j} I_{\lambda(i),\alpha(j)} - \kappa \cdot S^2\{I_{\lambda(i),\alpha(j)}\} \tag{S2}$$

The image height is analytically predicted using Eq. 1 in the main text. $I_{\lambda(i),\alpha(j)}$ is the intensity at the analytically predicted focal spot at the wavelength $\lambda(i)$ and angle-of-incidence (AOI) $\alpha(j)$. The summation is carried out over the target spectral range 1-1.2 $\mu$m with 0.01 $\mu$m sampling spacing and 180° FOV with 10° sampling spacing. $\kappa$ is again set to 0.5 to reduce performance variance among different wavelengths and AOIs.

The DS optimization starts with generating a random initial phase mask of metalens. The algorithm then traverses all meta-atom positions, replacing the meta-atom with a different meta-atom structures from the library each time and computing the FOM using the Kirchhoff diffraction integral. The meta-atom design with the largest FOM is selected before moving on to the next meta-atom position on the metasurface. The process proceeds till the entire metasurface is traversed.

For the achromatic metalens in our first example, azimuthal symmetry of the optical system allows the Kirchhoff diffraction integral to be performed only along the radius of the metalens. For the broadband wide FOV metalens, the metasurface is divided into a set of concentric rings. The diffraction integrals from meta-atoms in each concentric ring region are computed and stored before the DS optimization. The "partial" integral values are reused and constantly updated when a meta-atom is replaced throughout the optimization to drastically reduce the computational load.

## 3. CONFIGURATION OF BROADBAND AND WIDE-FOV METALENS

Fig. S3 illustrates the configuration of the broadband 'fisheye' metalens, comprising a flat transparent substrate with an aperture on the top surface and a metasurface patterned on the bottom

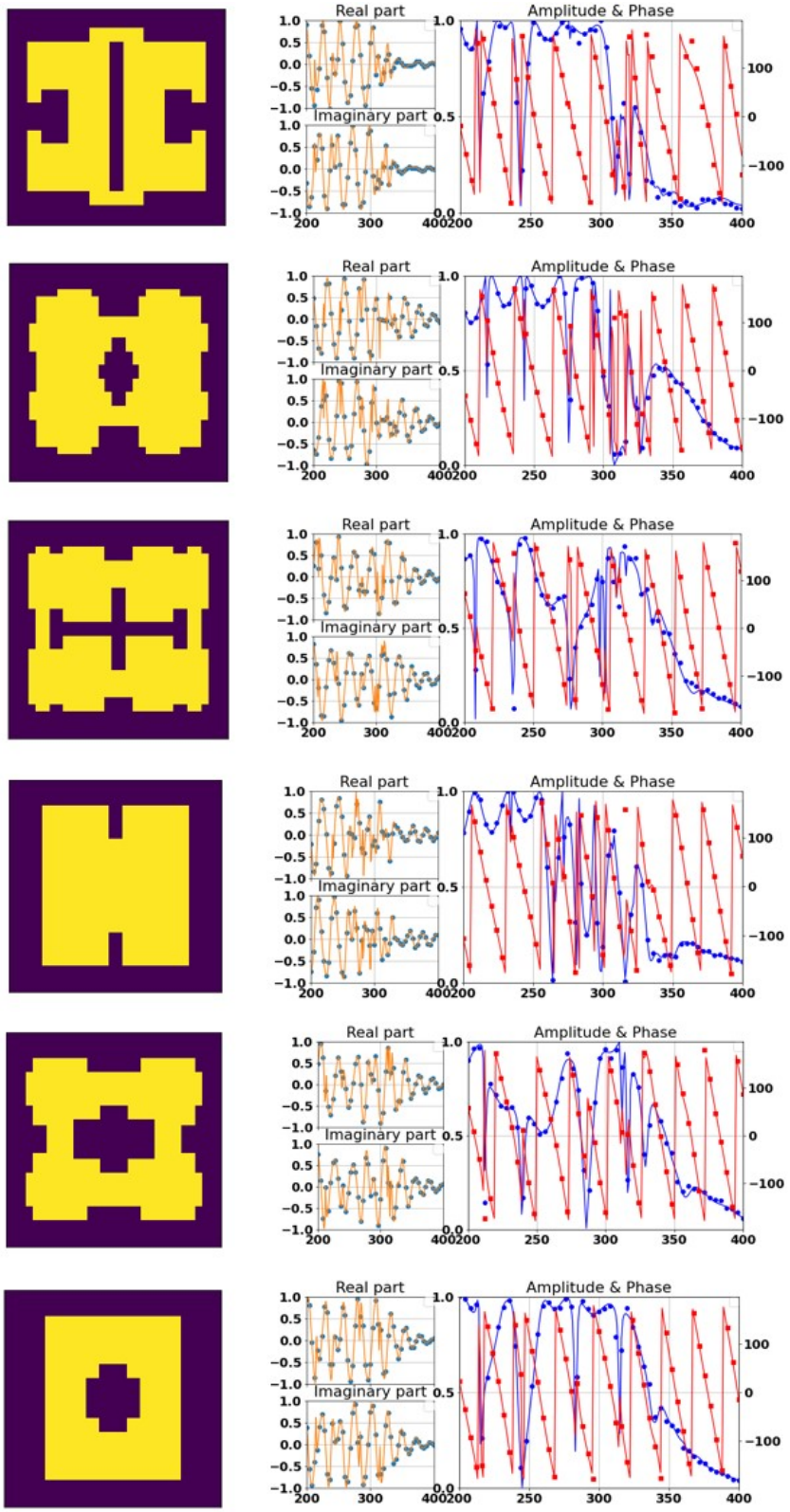


**Fig. S1.** Examples of meta-atom structures top-view, and their amplitude and phase response using full-wave simulations (lines) and the deep neural network (dots).

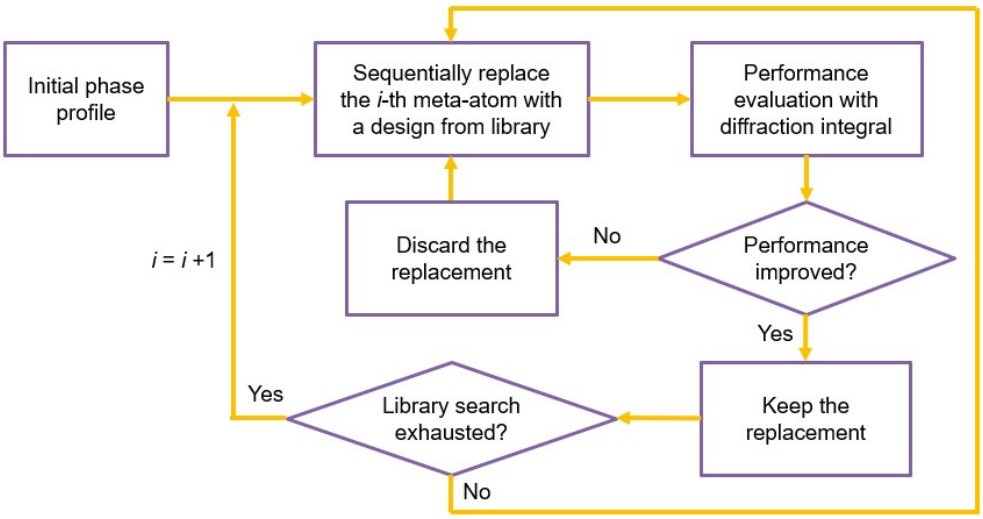


**Fig. S2.** Flow chart of DS algorithm.

surface[1]. Beams from different AOIs are refracted at the top surface and arrive at different and yet continuous portions of the backside metasurface. To achieve achromatic operation, beams of different wavelengths but with the same AOI must focus onto the same focal spot.

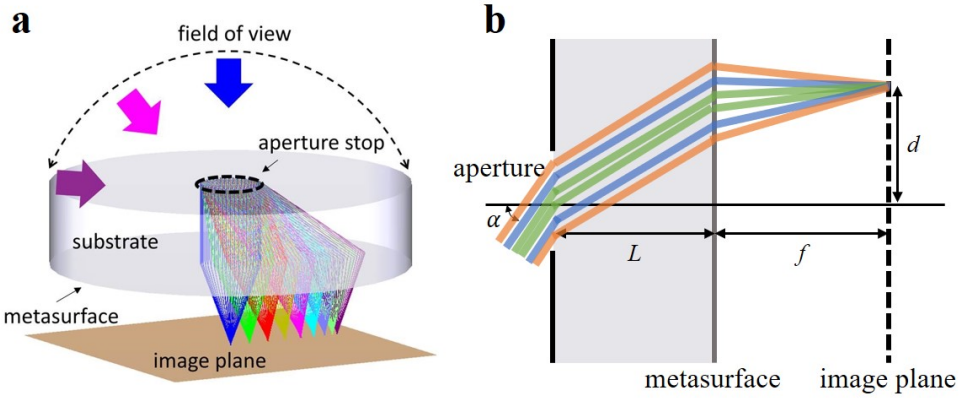


**Fig. S3.** Schematic illustration of broadband and wide-FOV metalens design. (a) 3-D structure. (b) Beams of different wavelengths all focus at the same focal spot with distance $d$ (image height) depending on AOI $\alpha$.

## 4. TRANSVERSE CHROMATIC ABERRATION

Eq. 1 in the main text predicts the focal spot's transverse position at a single wavelength relative to the optical axis. For broadband lenses, the focal spot position is wavelength dependent, resulting in transverse chromatic aberration. Fig. S4 presents the axial intensity distribution at different wavelengths and AOIs for a wide-FOV lens optimized for single-wavelength operation at 1.1 $\mu$m. In addition to the axial chromatic focal shift, the focal spot moves toward the optical axis in the transverse direction as wavelength increases and vice versa. Such transverse chromatic focal shift aka transverse chromatic aberration becomes more pronounced as the AOI increases. Therefore, this effect is only significant in wide-FOV achromatic metalenses and little attention has been paid to this effect before. The transverse chromatic aberration can be mitigated by reducing the spectral bandwidth or the FOV. Fig. S5 illustrates the trade-off between bandwidth and FOV: for

the same level of transverse chromatic aberration, the FOV must be curtailed as the bandwidth increases.

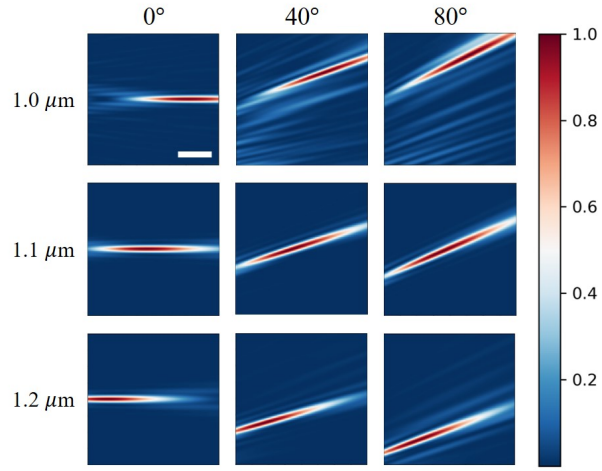


**Fig. S4.** Axial intensity distributions on the meridional plane of a wide-FOV lens at different wavelengths and AOIs (scale bar: 20 $\mu$m). The lens is optimized for single-wavelength operation at 1.1 $\mu$m. Centers of the figures are the analytically predicted focal spot positions on image plane from Eq. 1 in the main text.

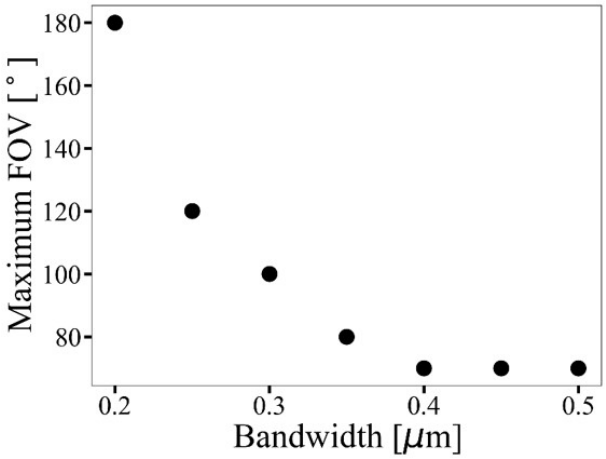


**Fig. S5.** Maximum achievable FOV as a function of the metalens bandwidth for a fixed level of transverse chromatic aberration. The lower end of the wavelength is set at 1 $\mu$m.

## 5. COMPARISON OF META-ATOM OPTIMIZATION ALGORITHMS

In the main text, we describe an optimization protocol where the optimal meta-atom is selected from a library comprising 3,000 free-form meta-atom designs randomly generated using a needle-drop technique during the DS process. This approach leaves two open questions: one is that whether the meta-atom library is sufficiently to cover all geometric variants to attain optimal performance; and the second question is whether the optical performance of final metalens design approaches that of the global optimum, since the DS algorithm tends converge upon local optima. To address the questions, we explored additional optimization algorithms and parameter sets.

First, the DS optimization process was repeated multiple times with the same meta-atom library but different (randomly generated) initial phase profiles. The optimized focusing efficiencies and Strehl ratios generally differ by only a few percent. The outcome suggests that while the DS

algorithms converge to different local optima, the optical performances associated with the local optima (and likely the global optima as well) are relatively similar.

We then executed the same DS optimization process but with several other libraries, each comprising a different set of 10,000 randomly generated meta-atoms. The best result from the trials is included in Table S1 below. We notice that the performance obtained with the 10,000 meta-atom library is similar to that with the original 3,000 meta-atom library, indicating that further expanding the library only brings marginal benefits.

To ensure adequate coverage of the free-form meta-atom design space, we further experimented with an alternative meta-atom layout generation scheme, the surface contour method proposed by Whiting *et al.*[2]. The main advantage of this method is that a free-form meta-atom shape can be specified with a small number of parameters (i.e. the heights of control points which define the contour). In each of the meta-atom substitution step during the DS optimization, 1,000 meta-atoms were first randomly generated using the surface contour method. The meta-atom that yields the best performance upon substitution was selected. Subsequently, the selected meta-atom design (as specified by the control point heights) was further optimized using a gradient-descent algorithm before moving onto the same substitutional operation on the next meta-atom.

Table S1 compares the optical performances (focusing efficiency and Strehl ratio averaged over the 1-1.5 $\mu$m band) of metalenses optimized using the aforementioned approaches. Since all approaches lead to similar results, we conclude that the method presented in the main text is the preferred optimization scheme given its minimal computational overhead compared to other alternatives.

**Table S1. Comparison between different optimization algorithms**

| Optimization algorithm | Focusing efficiency | Strehl ratio |
|---|---|---|
| 3,000 meta-atom library | 42% | 0.67 |
| 10,000 meta-atom library | 46% | 0.67 |
| Surface contour method + gradient descent | 44% | 0.59 |

## 6. ACHROMATIC METALENS PERFORMANCE BENCHMARCK

In the work by Presutti *et al.*[3], bandwidth limits have been derived which elucidates the trade-off between bandwidth and numerical aperture (NA). Comparisons were also drawn among published achromatic metalens results. Here we quote their comparison chart and benchmark our lens performance against other reports, as shown in Fig. S6. For our design, $n_b = 1$ is the background refractive index, $\Delta\omega$ is the operational bandwidth, $F$ is the focal length, $c$ is the speed of light, and $\kappa$ is a dimensionless quantity ($\kappa = 2$ for metasurfaces with a deep subwavelength thickness). The chart indicates that our design offers the best-in-class spectral coverage for the given NA value. This is an important advantage of the DS approach presented here, since the optimization does not adhere to a phase profile defined *a priori* to maximize phase coherence at the focal spot. Instead, by leaving phase as a free parameter, we expand the design space which leads to enhanced performances.

## REFERENCES


1. M. Y. Shalaginov, S. An, F. Yang, P. Su, D. Lyzwa, A. M. Agarwal, H. Zhang, J. Hu, and T. Gu, "Single-element diffraction-limited fisheye metalens," Nano Lett. **20**, 7429–7437 (2020).
2. E. B. Whiting, S. D. Campbell, L. Kang, and D. H. Werner, "Meta-atom library generation via an efficient multi-objective shape optimization method," Opt. Express **28**, 24229–24242 (2020).
3. F. Presutti and F. Monticone, "Focusing on bandwidth: achromatic metalens limits," Optica **7**, 624–631 (2020).

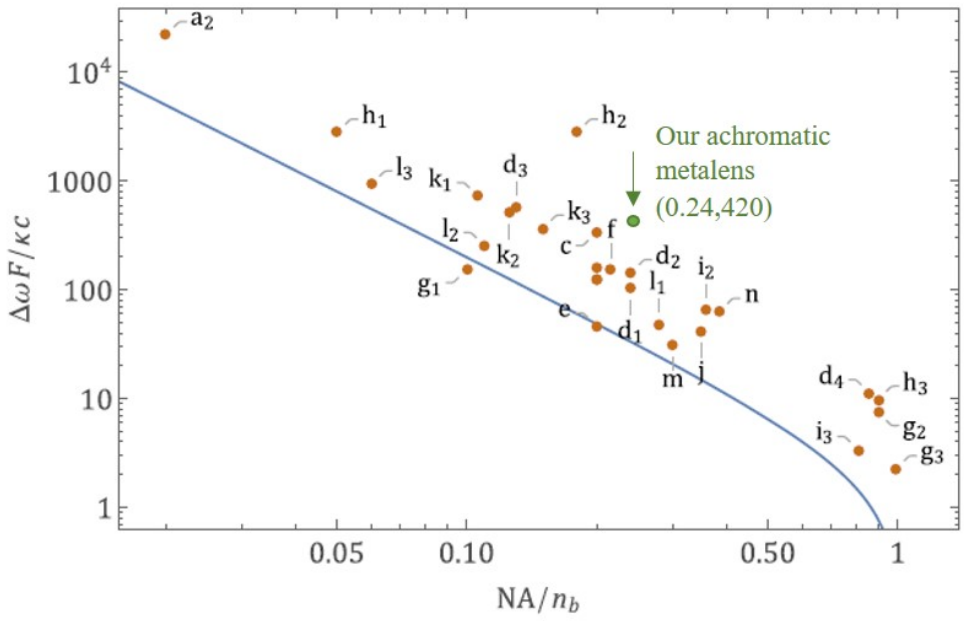


**Fig. S6.** Performance benchmark between published achromatic metalens designs. Reproduced from [3].